ACS APPLIED MATERIALS & INTERFACES

Research Article

www.acsami.org

Application of Organophosphonic Acids by One-Step Supercritical CO_2 on 1D and 2D Semiconductors: Toward Enhanced Electrical and Sensing Performances

Bhavesh Bhartia,[†,‡] Nadav Bacher,[†,§] Sundaramurthy Jayaraman,[†,⊥] Salam Khatib,[§] Jing Song,[∥] Shifeng Guo,[∥] Cedric Troadec,*[,∥] Sreenivasa Reddy Puniredd,*[,∥] Madapusi Palavedu Srinivasan,*[,‡] and Hossam Haick*[,§]

[‡]Department of Chemical and Biomolecular Engineering, National University of Singapore,4 Engineering Drive 4, Singapore 117585, Singapore

[§]The Department of Chemical Engineering and Russell Berrie Nanotechnology Institute, Technion−Israel Institute of Technology, Haifa 3200003, Israel

[⊥]Environmental and Water Technology Centre of Innovation, Ngee Ann Polytechnic, 535 Clementi Rd, Singapore599489, Singapore

[∥]Institute of Materials Research and Engineering, A*STAR (Agency for Science, Technology and Research), 3 Research Link, Singapore 117602, Singapore

Supporting Information

ABSTRACT: Formation of dense monolayers with proven atmospheric stability using simple fabrication conditions remains a major challenge for potential applications such as (bio)sensors, solar cells, surfaces for growth of biological cells, and molecular, organic, and plastic electronics. Here, we demonstrate a single-step modification of organophosphonic acids (OPA) on 1D and 2D structures using supercritical carbon dioxide ($SCCO_2$) as a processing medium, with high stability and significantly shorter processing times than those obtained by the conventional physisorption-chemisorption method (2.5 h vs 48−60 h).The advantages of this approach in terms of stability and atmospheric resistivity are demonstrated on various 2D materials, such as indium−tin-oxide (ITO) and 2D Si surfaces. The advantage of the reported approach on electronic and sensing devices is demonstrated by Si nanowire field effect transistors (SiNW FETs), which have shown a few orders of magnitude higher electrical and sensing performances, compared with devices obtained by conventional approaches. The compatibility of the reported approach with various materials and its simple implementation with a single reactor makes it easily scalable for various applications.

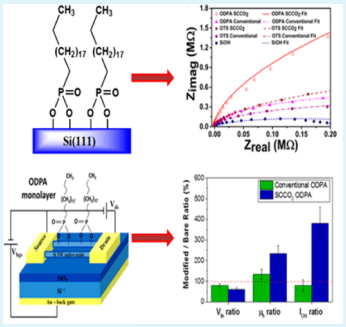

KEYWORDS: *supercritical carbon dioxde, organophosphonic acid, silicon nanowire, volatile organic compound, sensor, modification*

INTRODUCTION

Organic functionalization of surfaces is a key component of many emerging device applications that rely on single or a small group of organic molecules as functional building blocks of (opto)electronic circuits, solar cells, (bio)sensors, etc.[1−10] So far, the most common organic functionalization on semiconductors (e.g., via siloxanes) or metals (e.g., via thiols) have been limited to solution-processable species. As a result, the efficiency and/or performance of the consequent devices have been hindered by several factors, such as water/solvent content in the surface modification, age of the solution, long time for completing the modification, the need for postmodification cleaning, etc.[11] A promising candidate that has a potential to waive many of these restrictions is the organophosphonic acid (OPA) monolayer.[12−14] In comparison with common monolayers, such as silanes and thiols, OPA monolayers have a better surface coverage, no self-polymerization at ambient conditions and better hydrolytic stability in alkaline conditions.[15,16] As a result, OPA has raised expectation to give rise to robustly grafted uniform monolayers,[17] exhibit superior hydrolytic and thermal stability than siloxanes, and display better resistance to mechanical stress, which is important in determining device lifetime for biosensors,[18] molecular,[19] and organic electronics.[20,21] On top of these expected advantages, OPA monolayers can form stable, covalently bound self-assembled monolayers (SAMs) on various metal oxide surfaces used in organic electronics[20,21] and biosensor applications,[22] such as aluminum oxide (Al_2O_3),[12,23] mica,[24] titanium dioxide (TiO_2),[16,25] indium tin oxide (ITO),[26−28] or zinc oxide (ZnO).[29,30]

Conventionally, phosphonate molecules are attached to SiO_2 or ITO using tethering by aggregation and growth (T-BAG).[17,31] In this T-BAG process, phosphonic acid is initially weakly physisorbed for 12 h from a solution on the oxide

Received: April 25, 2015
Accepted: June 19, 2015
Published: June 19, 2015

DOI: 10.1021/acsami.5b03597
ACS Appl. Mater. Interfaces 2015, 7, 14885−14895

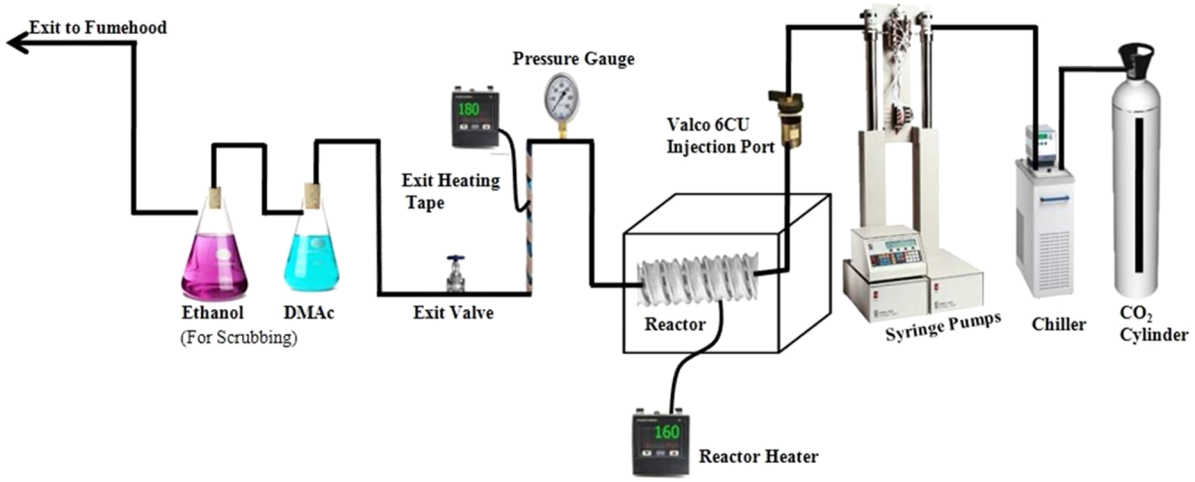

Figure 1. Schematic representation of $SCCO_2$ process.

substrate, forming a reasonably well-ordered layer. Then the formed layer is chemically attached by thermal treatment during which Si−O−P or In−O−P bonds are formed, respectively. This process usually extends over 48 h[17,32] and the removal of the unreacted phosphonic acid from the surface is not fully guaranteed.[33−35] Recent advancements in the T-BAG method can reduce the processing time to few hours; however, it demands very stringent humidity conditions during the processing.[14]

For Al_2O_3[21,36] and TiO_2[16,20,37] surfaces, the processing time for surface modification by the phosphonic acid requires at least 16−24 h. On top of these limitations, both the T-BAG processing as well as the quality of the resulting modification is strongly dependent on the environment as well as in the humidity level.

In this work, we report a one-step supercritical carbon dioxide ($SCCO_2$) procedure as a cost-effective and environmentally benign processing method[38,39] for chemisorption of highly dense and highly stable OPA monolayer with shorter processing time - see Figure 1. We demonstrate this approach on Si surfaces, being a representative material for a wide range of applications. $SCCO_2$ offers potential advantage over conventional processes because of its physical properties.[39−42] Short processing time as mentioned above for $SCCO_2$ process is due to high diffusivity of molecules in $SCCO_2$ as compared to conventional liquid-based methods.[43,44] Moreover, the ability to control the density by varying the pressure and temperature, makes $SCCO_2$ process highly adaptable to various other monolayers too.[44]

In the case of OPA SAM attachment on the silicon surface, the mechanism of deposition remains same as in the case of conventional method[17,31] but the difference between conventional and $SCCO_2$ process lies in the processing of physisorbed/chemisorbed OPA molecules. In conventional method, physisorption takes place first followed by heating to chemisorb the molecules on the surface. However, in $SCCO_2$ process, both steps, i.e., physisorption and chemisorption are carried out simultaneously, which significantly decreases the processing time. In conventional process, during the physisorption step, apart from ordered, self-assembled monolayer of OPA molecules, there are disordered multilayers also present on the surface due to the longer duration of physisorption process and also the low transport properties of the conventional medium.[17] After the chemisorption process, these multilayers are removed using an extensive rinsing process that is detrimental to the the quality of monolayer present underneath,[17,41] whereas in the case of $SCCO_2$ process, apart from favorable monolayer deposition conditions, multilayer formation is minimized by continuous removal of unreacted molecules from reactor before they can form multilayers, the short processing time and high transport properties of the $SCCO_2$, thus allowing post cleaning of the monolayer and formation of robust monolayers. The utility of the $SCCO_2$ technology is further extended to silicon nanowire field-effect transistors (SiNW FETs), ITO surfaces, and sensing of volatile organic compounds (VOCs).

EXPERIMENTAL METHODS

ODPA, OTS, and PFBpA Grafting by Conventional Solution Processing. The phosphonate molecules were grafted on 2D silicon and 1D SiNW FETs using a method called tethering by aggregation and growth or T-BAG.[17,31,45] Piranha-treated 2D wafers and plasma treated SiNW FET substrates were placed vertically upright in a 1 mM ODPA solution (below its critical micelle concentration) in tetrahydrofuran (THF) without stirring, with the aid of a sample holder. The solution was left to stand until THF evaporated completely, typically for 12 h. Subsequently, the wafers were heated in an oven at 140 °C for 48 h under N_2, sonicated in 0.5 M K_2CO_3 in 2:1 ethanol/water ("carbonate rinse") for 10 min to remove any ODPA multilayer, sonicated for 5 min in fresh THF, rinsed copiously in deionized water and finally dried in a stream of dry N_2. The substrates containing the 1D SiNW FETs were successively rinsed in 0.5 M K_2CO_3 in 2:1 ethanol/water and fresh THF for 5 min each, washed with deionized water and dried with N_2. OTS was deposited on 2D silicon and 1D SiNW FETs as reported earlier.[46] For 2,3,4,5,6-pentafluorobenzylphosphonic acid (PFBpa) grafting on ITO, cleaned ITO samples placed vertically in 1 mM solution of PFBpa in THF solution and allowed to evaporate, depositing physically adsorbed multilayer of PFBpa on ITO. To chemically adsorb the molecules, we then heated the sample at 140 °C for 48 h in a N_2(g) atmosphere. Physically adsorbed multilayer of PFBpA samples were washed with 10 min sonication in 5% triethylamine in THF, followed by extensive rinsing with DI water and drying with N_2(g).

ODPA, OTS, and PFBpA Grafting by $SCCO_2$ Approach. The supercritical fluid (SCF) process was conducted in a system schematically depicted in Figure 1. A 20 mm I.D. × 140 mm length stainless steel column was used to house the wafer samples. The column containing the hydroxyl terminated 2D silicon substrates and plasma activated SiNW FETs were contacted with a heating coil coupled with a thermocouple and held at temperature of 140 °C and exposed to 10 MPa of $SCCO_2$ (pressurized by means of an ISCO

DOI: 10.1021/acsami.5b03597
ACS Appl. Mater. Interfaces 2015, 7, 14885−14895

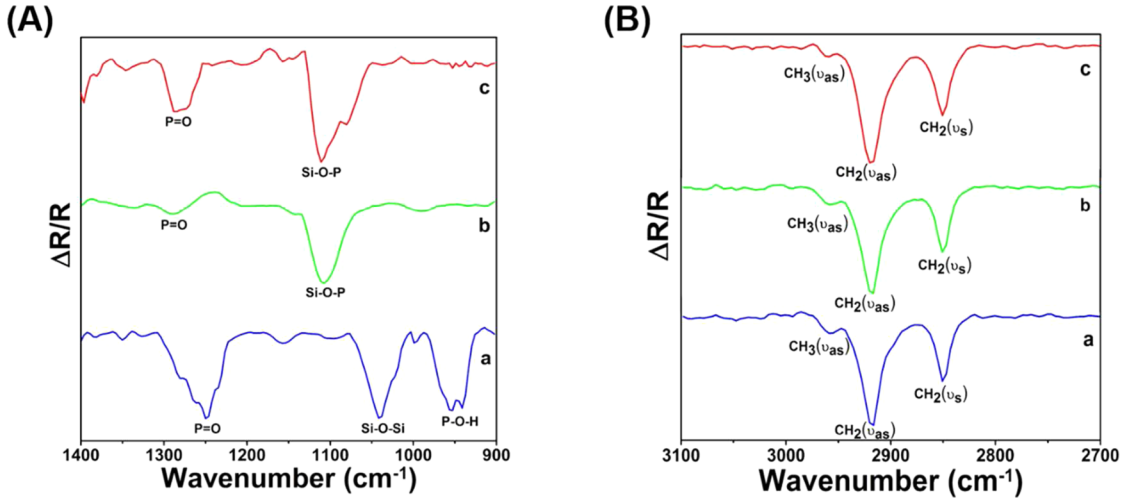

Figure 2. FTIR spectra for (A) phosphonate and (B) aliphatic region of ODPA (octadecylphosphonic acid) deposited by different processing approaches: (a) physically adsorbed, (b) conventional process, and (c) $SCCO_2$ process (FTIR spectra were plotted as change in reflectance of substrate with respect to background ($\Delta R/R$) vs. wavenumber).

syringe pump) at a flow rate of 0.25 mL/min. Five mM of the ODPA and PFBpA in THF solvent were injected into the CO_2 stream through a six-way chromatography valve (Valco) for respective silicon and ITO surfaces. For OTS deposition, reactor was kept at 40 °C and 10 MPa, and deposition was carried out using 5 mM solution of OTS in toluene. Four successive injections (1 mL/injection) of the solution at 30 min intervals were performed followed by 30 min flushing of reactor with fresh $SCCO_2$ to remove any physisorbed layer on the surface. Column was depressurized after the final injection over a period of 30−45 min.

RESULTS AND DISCUSSION

Understanding the effect of the processing properties as well as the type of the bond(s) associated with SAM formation is of critical importance for designing protocols that could be implemented in practical applications. With this in mind, we have compared the formation of octadecylphosphonic acid (ODPA) from phosphonate and octadecyltrichlorosilane (OTS) on Si/SiO_2 surfaces and from 2,3,4,5,6-pentafluorobenzylphosphonic acid (PFBpA) on ITO surfaces. The properties of the resulting films when $SCCO_2$ is deployed as the processing vehicle were compared to the use of liquid solvent with the same molecules of interest.

Fourier-transform infrared spectroscopy (FTIR) was performed to investigate the changes in chemical bonds at the silicon oxide interface. Figure 2A, B shows the reflectance spectra as a function of processing method. Figure 2A-a shows all of the typical spectral features of a fully protonated physisorbed phosphonic acid: the stretch mode of the (P═O) at 1235 cm^{-1}, the asymmetric and symmetric stretch modes of the (P═O) at 1078 and 1004 cm^{-1}, and the deformation mode of the (P−O−H) at 956 cm^{-1}.[14,17,47] In the aliphatic region, (Figure 2B-a) the broad spectral positions of the strong asymmetric and symmetric stretch modes of the ($-CH_2-$) at 2915 and 2850 cm^{-1} respectively and asymmetric stretch mode of the ($-CH_3$) at 2960 cm^{-1}, indicate that the physisorption step takes advantage of the arrangement of amphiphilic molecules at the liquid/gas interface.[14]

The FTIR spectrum in Figure 2A-b shows the resulting IR spectrum at the end of the conventional process after heating the physically adsorbed ODPA at 140 °C for 48h and followed by cleaning. The presence of the (P═O) mode at 1250 cm^{-1}rules out the formation of the primarily tridentate bonding and the absence of the (P−O−H) mode at 956 cm^{-1} rules out the monodentate configuration. The formation of a chemical bond to the surface is evident in the presence of the (Si−O−P) stretch mode at 1108 cm^{-1}, which can directly support the bidentate bonding configuration, although the surface is far from being homogeneous.[14] On the other hand, $SCCO_2$ processed ODPA film (Figure 2A-c) shows an additional weak signal at 1080 cm^{-1}.The specific frequencies, strong mode at 1108 cm^{-1} and a weaker shoulder at 1080 cm^{-1}, directly support the bidentate bonding configuration similar to that obtained by the conventional method. The presence of the sharp spectra of symmetric and asymmetric stretch mode of ($-CH_2-$) at 2918 and 2850 cm^{-1}, respectively, and asymmetric stretch mode of ($-CH_3$) at 2960 cm^{-1} (Figure 2B-c, B-b) are suggestive of the formation of ODPA films.[5,17] Furthermore, to confirm the chemisorption of monolayers, as deposited monolayers were sonicated in their respective solvent for 5 min to observe any changes in the contact angle and it remains same for both the $SCCO_2$ and T-BAG monolayers.

In addition to FTIR, X-ray photoelectron spectroscopy (XPS) analysis was also carried out to confirm the presence of phosphonate heads on the silicon dioxide interface. High resolution XPS spectra of P 2s of ODPA monolayer on Si/SiO_2, deposited by $SCCO_2$ process and conventional process, are shown in the Supporting Information, Figure 3S and was compared with ODPA powder for reference. Peak, at binding energy of 191.5 eV is attributed to P 2s of phosphonate group and peak at 184 eV is attributed to silicon plasmon peak, as shown in the Figure 3S in the Supporting Information and these peaks are similar to the reported literature.[48,49] For further information, see the Supporting Information, Section 2.2.

Spectroscopic ellipsometry analysis confirmed the presence of the ODPA molecules on silicon surfaces and yielded average film thicknesses of 2.6 ± 0.2 nm in the case of the $SCCO_2$ process and 2.4 ± 0.2 nm in the case of the conventional deposition process.[17,19,50] Contact angles at ambient temperature of the ODPA on silicon and PFBpA on ITO were, respectively, 110 ± 2° and 98 ± 2°in the case of $SCCO_2$ process and 90 ± 2° and 82 ± 2°in the case of the conventional

DOI: 10.1021/acsami.5b03597
ACS Appl. Mater. Interfaces 2015, 7, 14885−14895

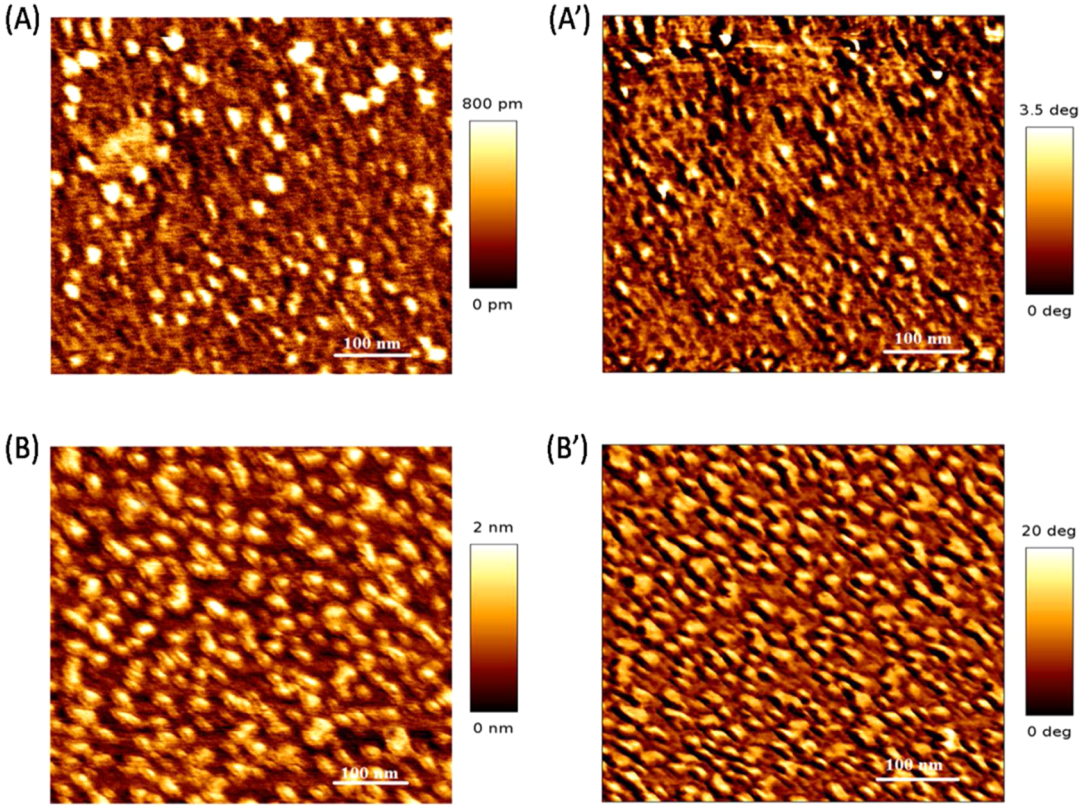

Figure 3. Tapping mode height (left panel) and phase (right panel) AFM images of the ODPA modification SAMs by (A) conventional (height); (A′) conventional (phase); (B) $SCCO_2$ (height); and (B′) $SCCO_2$ (phase).

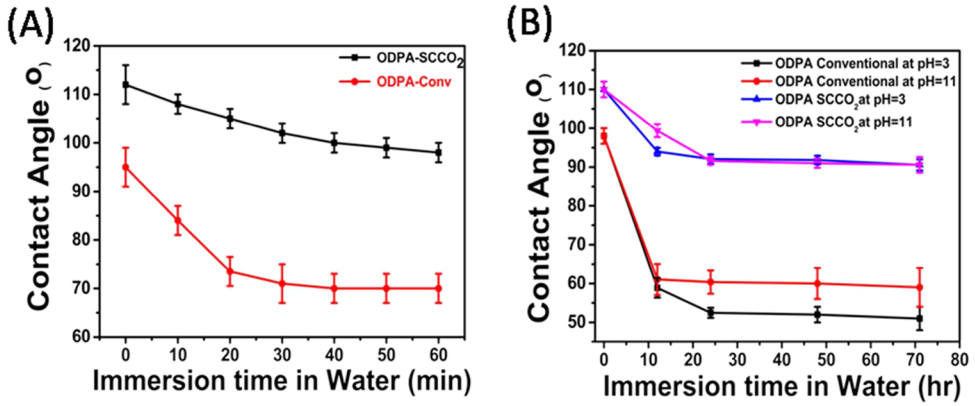

Figure 4. (A) Hydrolytic stability, and (B) acidic and basic stability of ODPA monolayer, deposited from the conventional and $SCCO_2$ process.

process.[19,51] The observation of the higher contact angles in the $SCCO_2$ case indicate that this processing approach gives a more organized and dense monolayer compared to that obtained by the conventional process.

AFM analysis (Figure 3A, A′, B, B′) shows distinct differences in the surface morphology when different processing mediums are used. The morphology of ODPA SAM grown by conventional processes is not uniform and, in general, the surface features of the films are composed of pinholes with smeared out topography (Figure 3A, A′). In contrast, the surface modification prepared by the $SCCO_2$ process revealed sharper features and small regular domains with a fairly uniform morphology (Figure 3B, B′) suggesting that the monolayer assembly is more organized. For the sake of comparison with more common SAMs, similar differences in morphology are also observed for OTS modified surfaces in both conventional and $SCCO_2$ processes—see the Supporting Information, Figure 1S. The differences in the morphologies might be due to the different transport properties of the conventional and $SCCO_2$ mediums, suggesting that the $SCCO_2$ process may have aided the nearly vertical and dense packing of the ODPA molecules.[41]

To further study the quality of ODPA monolayers in both the conventional and $SCCO_2$ processes, we have investigated their hydrolytic stability at room temperature with constant agitation in three different aqueous media containing deionized water, an acidic (HCl) solution at pH 3, and a basic (NaOH) solution at pH 11 as a function of immersion time. The samples were removed from the above solutions after different time intervals, cleaned copiously with deionized water, dried with N_2(g), and their static water contact angles were measured. The

DOI: 10.1021/acsami.5b03597
ACS Appl. Mater. Interfaces 2015, 7, 14885−14895

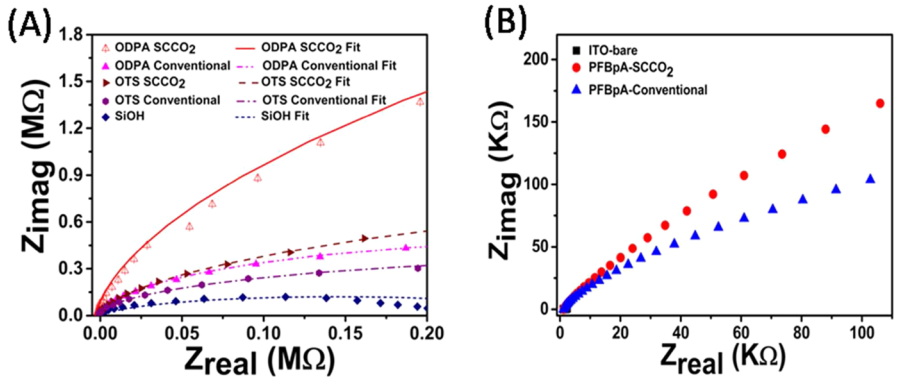

Figure 5. (A) Nyquist plots of the bare silicon oxide, ODPA, OTS (octadecyltrichlorosilane) SAMs deposited on silicon by $SCCO_2$ and conventional process. (B) Nyquist plots of the bare ITO, PFBpA (2,3,4,5,6-pentafluorobenzylphosphonic acid) SAM deposited on ITO by $SCCO_2$ and conventional process.

resulting contact angle measurements are shown in Figure 4A, B. Clearly, for conventional SAMs, a significantly lower stability is observed compared to the $SCCO_2$ process in all three aqueous solutions. After prolonged immersion in aqueous medium, the rate of degradation of ODPA monolayer is ∼8−10% in the case of the $SCCO_2$ process and ∼30−45% in the case of the conventional process. $SCCO_2$-made ODPA films are equally stable in both acidic and basic environments, in contrast to the films prepared by the conventional process that have shown greater degradation in acidic pH. Decrease in contact angle under aqueous conditions is due to hydrolysis of surface bonds and removal of molecules from surface. As a result, there is a partial decrease in hydrophobic aliphatic chains on surface vis à vis decrease in contact angle. Pin holes present in the monolayer allows water molecules to reach the surface and hydrolyze the surface bond. Conventional monolayer with less uniform coverage and density, showed a larger decrease in contact angle as compared to denser and more uniform $SCCO_2$ monolayers. Kinetically, it is assumed that the quick initial drop in contact angle is due to hydrolysis of monolayers in the pinhole region and afterward attain a stable contact angle as the remaining monolayer is densely packed, hence cannot be hydrolyzed. Contact angles measured after 4 months showed a decrease from 110 to 102° for $SCCO_2$-processed ODPA films and from 98 to 82° for conventional films. This observation further confirms the enhanced monolayer density and stability obtainable by the $SCCO_2$ process.

Electrochemical impedance spectroscopy (EIS) was carried out on silicon surfaces covered with native oxide, and with ODPA and OTS monolayers bound to the surface with phosphonate (−Si−O−P) and silane (−Si−O−Si−) bonds, respectively (Figure 5A and 5B). Similar EIS analysis was carried out on ITO surfaces modified with PFBpA via phosphonate bond (−In−O−P) and prepared by both conventional and $SCCO_2$ processes. Both the conventionally and $SCCO_2$-processed films exhibited significantly higher electrochemical resistance compared to the bare samples. The electrochemical resistance for the $SCCO_2$-processed ODPA SAMs were generally higher than that for the corresponding conventionally processed ODPA and OTS films, because of the formation of denser ODPA films by the former process. The EIS data were further fitted with equivalent circuits as shown in the Supporting Information, Figure 2S. The resistance for the ODPA film deposited on silicon dioxide from $SCCO_2$ is 5 and 4 times higher than that obtained from the conventional ODPA and OTS films deposited from $SCCO_2$ processes on silicon, respectively. The resistance for the PFBpA deposited on ITO from $SCCO_2$ is also 2 times higher than the film prepared by the conventional process (Figure 5B).This observation clearly indicates that the $SCCO_2$-deposited phosphonate monolayer has a much lower number of surface defects and is thus of superior quality to that of the conventionally deposited phosphonate and silane monolayers for both the substrates.

On the basis of the aforementioned results, the $SCCO_2$ process was implemented on 1D nanostructure and related electronic devices. More specifically, back-gate FETs based on well-aligned SiNWs channels[52] between source and drain electrodes were fabricated and subsequently grafted with ODPA and OTS monolayers from conventional and $SCCO_2$ processes (see Experimental Methods). A schematic illustration of the ODPA modified SiNW FETs is shown in Figure 6A. Figure 6B, C demonstrates a comparison between the source-drain current (I_{ds}) versus back-gate voltage (V_{bgs}) characteristics (ranging from +40 to −40 V at source−drain voltage V_{ds} = 1 V) of SiNW FETs modified with ODPA and OTS using $SCCO_2$ process (blue line), conventional process (green line) and their respective unmodified devices (blue and green dots). The measured I_{ds}−V_{bgs} curves after ODPA and OTS modifications by both the conventional and $SCCO_2$ processes were shifted to the left and resulted in a lower threshold (turn on) voltage (V_{th}). The modification of SiNWs with the monolayers also influenced the hole-mobility (μ_h) and on-current (I_{ON}) of the devices compared to the unmodified (bare) devices. Devices modified with the $SCCO_2$ process showed superior transistor performances compared to devices modified with the conventional process and in addition, ODPA showed enhanced capabilities compared to the OTS.

Based on the I_{ds}−V_{bgs} characteristics, the fundamental V_{th}, μ_h, I_{ON} were calculated for all tested devices (see the Supporting Information, Section 2.7 for further details). The electrical parameters of the ODPA and OTS-SiNW FET series from both the conventional and $SCCO_2$ processes were compared with the respective unmodified devices. Generally, more significant shifts in V_{th}, μ_h, and I_{ON} values were observed for the $SCCO_2$ process compared to the conventional one (Figure 6D, E). Additionally, all SiNW FETs have shown a decrease in the threshold voltage ($\Delta V_{th} < 0$) after the attachment of the SAM (Figure 6F, G) V_{th} for control (bare) devices were typically between +22 V to +30 V, whereas SAM-modified devices consistently exhibited a lower V_{th} values. Devices modified with

DOI: 10.1021/acsami.5b03597
ACS Appl. Mater. Interfaces 2015, 7, 14885−14895

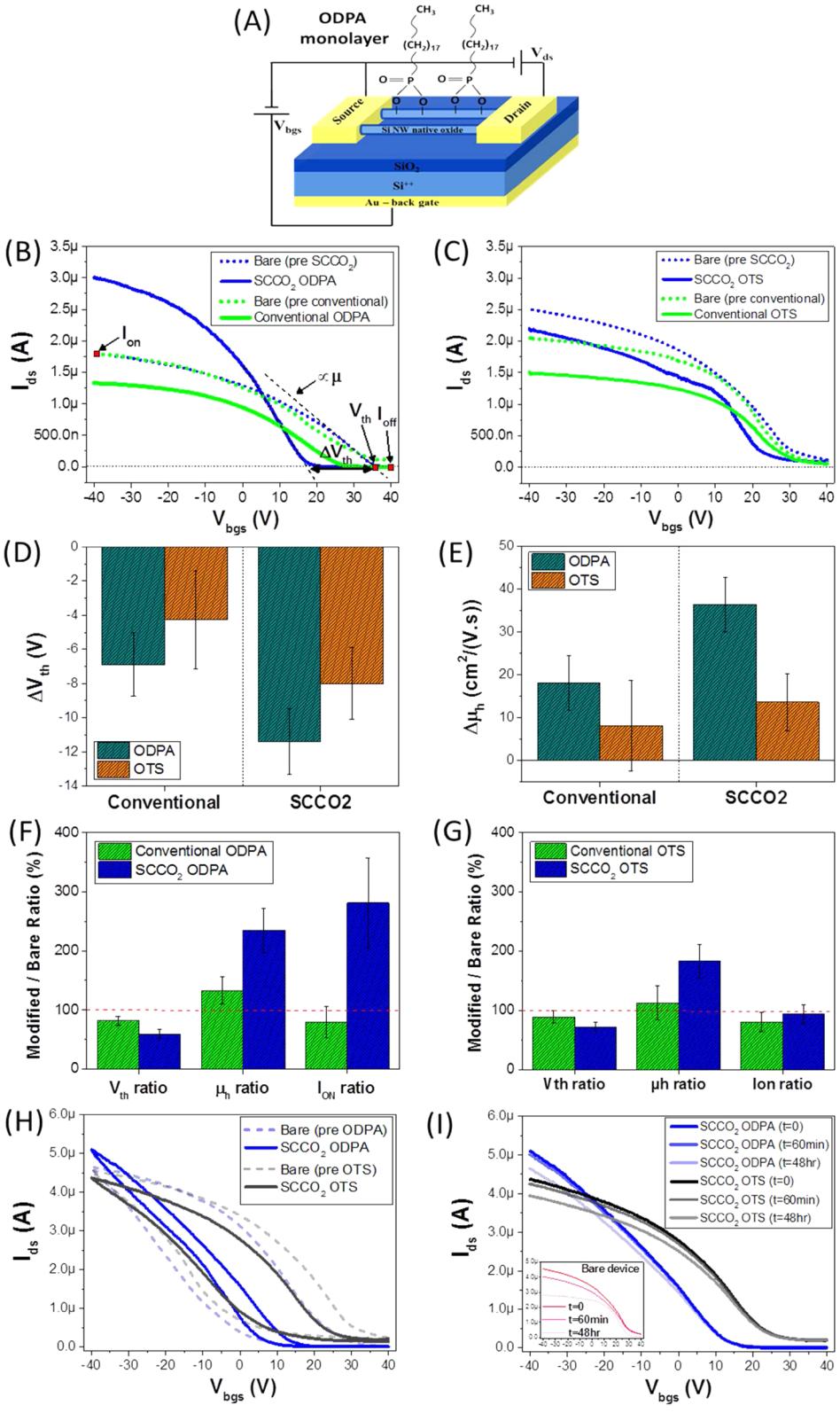

Figure 6. (A) Schematic representation of the ODPA-SiNW FET. Typical $I_{ds}-V_{bgs}$ curves of: (B) bare and ODPA-SiNW FET, and (C) bare and OTS-SiNW FETs, using conventional and $SCCO_2$ processes. The transistor parameters (V_{th}, μ_h, and I_{ON}) are marked in the figure. Changes in (D) V_{th}, (E) μ_h measured for the different ODPA and OTS modifications. The change in the threshold voltage (ΔV_{th}), hole-mobility ($\Delta\mu_h$) and on-current (ΔI_{ON}) were calculated by subtracting the parameter values measured before and after modification. Ratios of the fundamental electrical parameters between modified and bare devices due to the different (F) ODPA and (G) OTS modifications. (H) I_{ds}-V_{bgs} forward and backward sweeps of bare, $SCCO_2$ ODPA and $SCCO_2$ OTS SiNW FETs. (I) Stability characteristics over 48 h of bare, $SCCO_2$-made ODPA-SiNW FETs and $SCCO_2$ –made OTS-SiNW FETs. Note: The electrical characterization and analysis were performed on series of ten $SCCO_2$-made ODPA-SiNW FETs and OTS-SiNW FETs and on nine conventional ODPA-SiNW FETs and OTS-SiNW FET modified SiNW devices.

DOI: 10.1021/acsami.5b03597
ACS Appl. Mater. Interfaces 2015, 7, 14885−14895

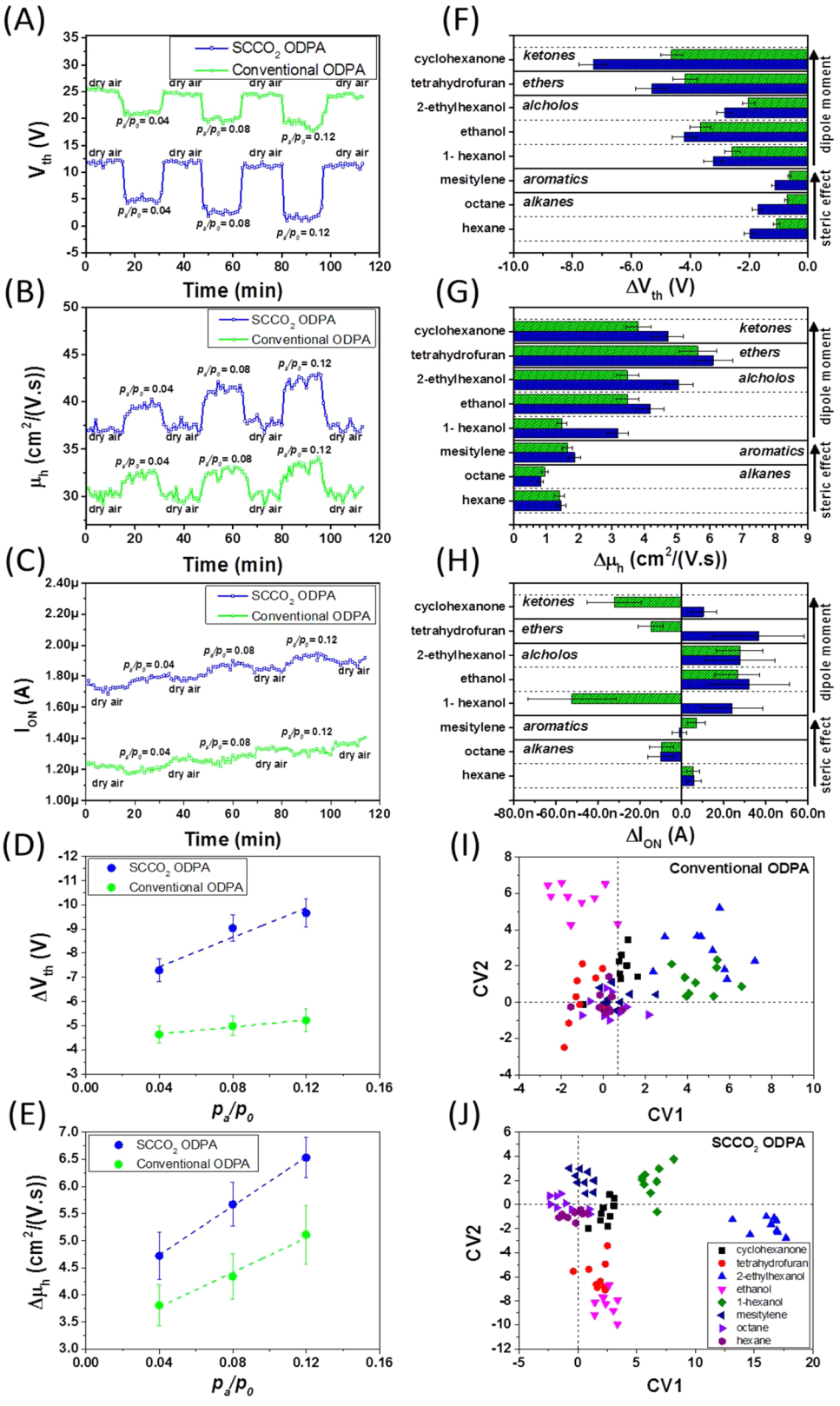

Figure 7. Time-dependent responses of conventional and $SCCO_2$ ODPA-SiNW FET sensors as expressed by (A) V_{th}, (B) μ_h, and (C) I_{ON} on exposure to cyclohexanone at different concentrations (p_a/p_o = 0.04, 0.08, and 0.12). Changes in (D) V_{th}, (E) μ_h of conventional and $SCCO_2$ ODPA-SiNW FET sensors vs cyclohexanone concentration. Changes in (F) V_{th}, (G) μ_h, and (H) I_{ON} of the sensors upon exposure to various VOCs at a representative concentration of p_a/p_o = 0.04 (an average of three repetitions for each VOC). DFA results separating between the various VOCs examined in the study (see the Supportin Information, Table 1S) at different concentrations (p_a/p_o = 0.04, 0.08, 0.12) using (I) seven $SCCO_2$-made ODPA-SiNW FET sensors and (J) seven ODPA-SiNW FET sensors by the conventional process.

DOI: 10.1021/acsami.5b03597
ACS Appl. Mater. Interfaces 2015, 7, 14885−14895

$SCCO_2$-made ODPA monolayer exhibited the lowest V_{th}, with typical values of +12 V, correspond to a ΔV_{th} of −11.5 ± 1.9 V or 59 ± 8% of the V_{th} of the respective unmodified (bare) devices. In comparison, these values were much lower than the conventional ODPA (ΔV_{th} of −6.9 ± 1.9 V or 82 ± 8%) and OTS modified devices (−8.0 ± 2.1 V or 72 ± 8% for device prepared with the $SCCO_2$ process and −4.3 ± 2.1 V or 87 ± 10% for devices prepared with the conventional process). Because V_{th} determines the requirements for turning the transistor on or off, devices with lower V_{th} require lower operating voltages and thus are more power efficient.

Some applications require not only a low value of V_{th}, but also a precisely controlled value to match other devices in the circuit. Hence, the ability to adjust the V_{th} of the device using the SAM modification process is highly essential. SAM deposition on the SiNWs has also increased the mobility of the devices ($\Delta\mu_h > 0$). $SCCO_2$-made ODPA devices, for example, exhibited the largest $\Delta\mu_h$ shift of 36.3 ± 6.3 $cm^2/(V\ s)$, which correspond to 235 ± 37% of the μ_h of the respective unmodified devices. For comparison, the similar device prepared by the conventional SAM process has displayed only 133 ± 22% (more details are shown in Figure 6). Assuming that the dipole moments and tilt angles are similar for both conventional and $SCCO_2$ processes, the higher packing density for the $SCCO_2$-made ODPA monolayer might explain the higher V_{th} and μ_h shifts (see the Supporting Information, Section 3, for further details). The on-currents (I_{ON}) of the $SCCO_2$-made ODPA-SiNW FETs were higher than the same device prepared by the conventional SAM process. The I_{ON} ratio for the $SCCO_2$-made SiNW FETs was considerably higher (281 ± 76%) than the SiNW FETs prepared by the conventional process (79 ± 27%). Lower I_{ON} values for ODPA-SiNW FETs prepared by the conventional ODPA process with respect to unmodified devices were also shown in the literature for pentacene-based organic transistors. This might be the result of leakage currents through the hybrid oxide/SAM dielectric.

Figure 6H shows the $I_{ds}-V_{bgs}$ characteristics, scanned forward (+40 to −40 V) and backward (−40 to +40 V) of SiNW FETs modified with ODPA and OTS using $SCCO_2$ process compared to their respective bare devices (prior to SAM deposition). Typically, the unmodified (bare) SiNW FETs showed large threshold voltage gap (ΔV_H) of about 25 to 30 V between the backward and the forward sweeps. Note: ΔV_H is widely accepted as a measure for the hysteresis, which originates from trap states on the SiNW native oxide surface.[46] This hysteresis (or ΔV_H) was reduced drastically to approximately 4 and 10 V after passivating the device using the $SCCO_2$ process with ODPA and OTS, respectively. The $I_{ds}-V_{bgs}$ characteristics of the $SCCO_2$ ODPA and OTS SiNW FETs remained highly stable over a period of 48 h as shown in Figure 6I and also for an overall period of 2 months (not shown).

The ODPA-SiNW FETs were used for sensing volatile organic compounds (VOCs), categorized as follows: alkanes (octane, hexane), alcohols (2-ethylhexanol, ethanol, 1-hexanol), ethers (tetrahydrofuran), aromatics (mesityelene) and ketones (cyclohexanone). The sensing responses to a single VOC were tested by introducing the VOC vapors to the sensors chamber with a 5 L/min constant flow. An exposure cycle included 15 min of air flow, followed by 15 min VOC vapors flow that was repeated three times at three successively increasing concentrations, from p_a/p_0 = 0.04 to 0.12 (where p_a stands for the partial pressure of the VOC and p_o stands for the saturated vapor pressure at 21 °C). Continuous $I_{ds}-V_{bgs}$ measurements were performed before, during, and after exposure to the VOCs by backward sweeping between +40 and −40 V with 200 mV steps and at 1 V_{ds} (see the Supporting Information, Section 2.7 for further details). As an illustrative example, time-dependent sensing parameters, for sensor response are shown in Figure 7A−C upon exposure of the SiNW FETs to cyclohexanone at different concentrations. The V_{th} response of both ODPA modified SiNW FET sensors were rapid, fully reversible, and sensitive to a wide range of concentrations. $SCCO_2$-made ODPA-SiNW FET sensor showed greater V_{th} responses to cyclohexanone (e.g., −7.3 ± 0.5 V for p_a/p_o = 0.04, where p_a stands for the partial pressure of the VOC and p_o stands for the saturated vapor pressure at 21 °C) than the ODPA-SiNW FET sensor prepared by the conventional process (−4.6 ± 0.4 V for the same concentration). As presented in Figure 7B, the changes in μ_h of the SiNW FET sensors due to cyclohexanone exposure were positive. Despite the slight increase in the baseline and noise level, the μ_h responses of the sensors were also significant and rapid (within less than 30 s). Again, $SCCO_2$-made ODPA-SiNW FET sensor showed larger response (e.g., 4.8 ± 0.3 $cm^2/(V\ s)$ for p_a/p_o = 0.04) than the ODPA-SiNW FET sensor prepared by the conventional process (3.9 ± 0.3 $cm^2/(V\ s)$ for the same concentration), yet not as substantial difference as for the V_{th} responses.

To evaluate the sensor sensitivity, V_{th} and μ_h responses were plotted versus cyclohexanone concentration as presented in Figure 7D, F, respectively. Our analysis suggests that V_{th} of the $SCCO_2$-made ODPA-SiNW FET sensor is 4 to 5 times more sensitive to variations in VOC concentrations than the ODPA-SiNW FET sensors prepared by the conventional process (represented by the sharper slope of the curve in Figure 7D). The slope of $\Delta\mu_h$ of the $SCCO_2$-made ODPA-SiNW FET sensor was found to be only 1.5 to 2 times larger than the conventional ODPA sensor. Each ODPA modified sensor has shown responses to a wide variety of VOCs as depicted in Figure 7D−F. Assuming that the dipole moments and tilt angles are similar for both conventional and $SCCO_2$ processes, the higher packing density for the $SCCO_2$ ODPA monolayer might act as response amplification factor and thus explain the higher V_{th} response to the various VOCs (see the Supporting Information, Section 4, for further details). An increase of $\Delta\mu_h$ upon exposure to VOCs was also reported previously for silane-terminated SiNW[26,46,53−55] and InAs NW FET-based gas sensors.[56] The increase in $\Delta\mu_h$ was attributed to a decrease in the density of the negatively charged surface states upon the adsorption of the VOCs.[53] Moreover, it has been proven that eliminating the trap groups, such as hydroxyl groups (OH), decreased the hysteresis effect and improved the sensing properties.[46] Therefore, the dependence of the $\Delta\mu_h$ response on the conventional and $SCCO_2$ processes might be due to the monolayer coverage and packing density of the monolayers as shown in AFM and EIS studies. The I_{ON} responses plotted in Figure 7H were not significant (less than 1% of the baseline current measured under dry air flow) and a clear trend cannot be established. Similar trends are also observed for other molecularly modified VOC sensors as shown in the literature.[26]

To demonstrate the effect of the reported process on the sensing capabilities of the SiNW FETs, we have evaluated the overall discriminative power of the ODPA-SiNW FET sensors prepared by both the conventional and $SCCO_2$ processes. For this end, predictive models were built for the $SCCO_2$ and

DOI: 10.1021/acsami.5b03597
ACS Appl. Mater. Interfaces 2015, 7, 14885−14895

conventional sensor arrays, using discriminant function analysis, DFA (see the Supporting Information, Section 2.8, for further details). Eight VOCs (see the Supporting Information, Table 1S), with three repetitions for each concentration (p_a/p_o = 0.04, 0.08, and 0.12) were used in the analysis. For this purpose, we have acquired the three independent FET sensing characteristics (ΔV_{th}, $\Delta\mu_h$, and ΔI_{ON}) per sensor as DFA input features. The corresponding classification accuracy of the DFA models were derived by leave-one-out cross validation. As shown in Figure 7I and 7J the $SCCO_2$-made ODPA-SiNW FETs sensor array provided better classification accuracy (= 93%) than the classification with ODPA-SiNW FET sensors array prepared by the conventional process (= 81%). Despite the large variation in VOC concentrations, the DFA plot obtained from the $SCCO_2$-made ODPA-SiNW FET sensors array showed tight clusters for each VOC and a clear separation between them (see the Supporting Information, Section 5, for further details).

SUMMARY AND CONCLUSIONS

This study presents a single-step $SCCO_2$ approach for modifying silicon and ITO surfaces with phosphonic acids that requires much shorter processing time as opposed to the physisorption-chemisorption method that is widely used today (2.5 h vs 48−60 h). The $SCCO_2$ processed monolayers exhibit superior ordering and higher packing density than those obtained by conventional solution processing. We have further shown that the $SCCO_2$ process can be extended to modification of SiNW FETs electrical devices and sensors as well as to ITO substrates. In all cases, surface modification via the $SCCO_2$[40,57] approach has shown completely higher performances than equivalent devices that are prepared by the conventional SAM approaches. The $SCCO_2$ modification process is a clean and environmentally benign process when compared to the conventional methods using liquid solvents. Furthermore, the entire process can be done in a single reactor, making it easily scalable. The universal appeal of this process can result in adaptation of the large, existent body of work in supercritical fluid deposition to the area of silicon and other 1D and 2D surface modifications. Further development of nanostructured materials and the ever-present demand toward further miniaturization will spur research activity in this area leading to the development of commercially attractive processes and protocols.

ASSOCIATED CONTENT

Supporting Information

Materials, methods, characterization, EIS analysis, XPS, VOC information, nanowire synthesis, device fabrication and characterization, electrical and sensing parameters calculation. The Supporting Information is available free of charge on the ACS Publications website at DOI: 10.1021/acsami.5b03597.

AUTHOR INFORMATION

Corresponding Authors

*E-mail: cedric-t@imre.a-star.edu.sg.
*E-mail: punitedds@imre.a-star.edu.sg.
*E-mail: chesmp@nus.edu.sg.
*E-mail: hhossam@technion.ac.il.

Author Contributions

†B.B., N.B, and S.J. contributed equally.

Notes

The authors declare no competing financial interest.

ACKNOWLEDGMENTS

Financial support from National University of Singapore in the form of a research scholarship for B.B. is gratefully acknowledged. S.R.P and C.T. acknowledge funding from IMRE, A*STAR.

REFERENCES

(1) Hotchkiss, P. J.; Jones, S. C.; Paniagua, S. A.; Sharma, A.; Kippelen, B.; Armstrong, N. R.; Marder, S. R. The Modification of Indium Tin Oxide with Phosphonic Acids: Mechanism of Binding, Tuning of Surface Properties, and Potential for Use in Organic Electronic Applications. *Acc. Chem. Res.* **2011**, *45*, 337−346.
(2) Ma, H.; Acton, O.; Hutchins, D. O.; Cernetic, N.; Jen, A. K.-Y. Multifunctional Phosphonic Acid Self-Assembled Monolayers on Metal Oxides as Dielectrics, Interface Modification Layers and Semiconductors for Low-Voltage High-Performance Organic Field-Effect Transistors. *Phys. Chem. Chem. Phys.* **2012**, *14*, 14110−14126.
(3) Zhang, B.; Qin, C.; Niu, X.; Xie, Z.; Cheng, Y.; Wang, L.; Li, X. On the Origin of Efficient Electron Injection at Phosphonate-Functionalized Polyfluorene/Aluminum Interface in Efficient Polymer Light-Emitting Diodes. *Appl. Phys. Lett.* **2010**, *97*, 043506.
(4) Yu, S.-Y.; Chang, J.-H.; Wang, P.-S.; Wu, C.-I.; Tao, Y.-T. Effect of Ito Surface Modification on Oled Device Lifetime. *Langmuir* **2014**, *30*, 7369−7376.
(5) Hofer, R.; Textor, M.; Spencer, N. D. Alkyl Phosphate Monolayers, Self-Assembled from Aqueous Solution onto Metal Oxide Surfaces. *Langmuir* **2001**, *17*, 4014−4020.
(6) Ghosh-Mukerji, S.; Haick, H.; Paz, Y. Controlled Mass Transport as a Mean for Obtaining Selective Photocatalysis. *J. Photochem. Photobiol., A* **2003**, *160*, 77−85.
(7) Haick, H.; Ambrico, M.; Ghabboun, J.; Ligonzo, T.; Cahen, D. Contacting Organic Molecules by Metal Evaporation. *Phys. Chem. Chem. Phys.* **2004**, *6*, 4538−4541.
(8) Shuster, G.; Gallimidi, Z.; Reiss, A. H.; Dovgolevsky, E.; Billan, S.; Abdah-Bortnyak, R.; Kuten, A.; Engel, A.; Shiban, A.; Tisch, U.; Haick, H. Classification of Breast Cancer Precursors through Exhaled Breath. *Breast Cancer Res. Treat.* **2011**, *126*, 791−796.
(9) Ermanok, R.; Assad, O.; Zigelboim, K.; Wang, B.; Haick, H. The Discriminative Power of Chemically Sensitive Silicon Nanowire Field Effect Transistors to Volatile Organic Compounds. *ACS Appl. Mater. Interfaces* **2013**, *5*, 11172−11183.
(10) Shehada, N.; Brönstrup, G.; Funka, K.; Christiansen, S.; Leja, M.; Haick, H. Ultrasensitive Silicon Nanowire for Real-World Gas Sensing: Noninvasive Diagnosis of Cancer from Breath Volatolome. *Nano Lett.* **2015**, *15*, 1288−1295.
(11) Chen, X.; Luais, E.; Darwish, N.; Ciampi, S.; Thordarson, P.; Gooding, J. J. Studies on the Effect of Solvents on Self-Assembled Monolayers Formed from Organophosphonic Acids on Indium Tin Oxide. *Langmuir* **2012**, *28*, 9487−9495.
(12) Thissen, P.; Valtiner, M.; Grundmeier, G. Stability of Phosphonic Acid Self-Assembled Monolayers on Amorphous and Single-Crystalline Aluminum Oxide Surfaces in Aqueous Solution. *Langmuir* **2009**, *26*, 156−164.
(13) Thissen, P.; Peixoto, T.; Longo, R. C.; Peng, W.; Schmidt, W. G.; Cho, K.; Chabal, Y. J. Activation of Surface Hydroxyl Groups by Modification of H-Terminated Si (111) Surfaces. *J. Am. Chem. Soc.* **2012**, *134*, 8869−8874.
(14) Vega, A.; Thissen, P.; Chabal, Y. J. Environment-Controlled Tethering by Aggregation and Growth of Phosphonic Acid Monolayers on Silicon Oxide. *Langmuir* **2012**, *28*, 8046−8051.
(15) Mani, G.; Johnson, D. M.; Marton, D.; Dougherty, V. L.; Feldman, M. D.; Patel, D.; Ayon, A. A.; Agrawal, C. M. Stability of Self-Assembled Monolayers on Titanium and Gold. *Langmuir* **2008**, *24*, 6774−6784.
(16) Silverman, B. M.; Wieghaus, K. A.; Schwartz, J. Comparative Properties of Siloxane Vs Phosphonate Monolayers on a Key Titanium Alloy. *Langmuir* **2005**, *21*, 225−228.

DOI: 10.1021/acsami.5b03597
ACS Appl. Mater. Interfaces 2015, 7, 14885−14895

(17) Hanson, E. L.; Schwartz, J.; Nickel, B.; Koch, N.; Danisman, M. F. Bonding Self-Assembled, Compact Organophosphonate Monolayers to the Native Oxide Surface of Silicon. *J. Am. Chem. Soc.* **2003**, *125*, 16074−16080.
(18) Cattani-Scholz, A.; Pedone, D.; Dubey, M.; Neppl, S.; Nickel, B.; Feulner, P.; Schwartz, J.; Abstreiter, G.; Tornow, M. Organophosphonate-Based Pna-Functionalization of Silicon Nanowires for Label-Free DNA Detection. *ACS Nano* **2008**, *2*, 1653−1660.
(19) Bora, A.; Pathak, A.; Liao, K.-C.; Vexler, M. I.; Kuligk, A.; Cattani-Scholz, A.; Meinerzhagen, B.; Abstreiter, G.; Schwartz, J.; Tornow, M. Organophosphonates as Model System for Studying Electronic Transport through Monolayers on Sio2/Si Surfaces. *Appl. Phys. Lett.* **2013**, *102*, 241602.
(20) Kraft, U.; Sejfić, M.; Kang, M. J.; Takimiya, K.; Zaki, T.; Letzkus, F.; Burghartz, J. N.; Weber, E.; Klauk, H. Flexible Low-Voltage Organic Complementary Circuits: Finding the Optimum Combination of Semiconductors and Monolayer Gate Dielectrics. *Adv. Mater.* **2014**, *27*, 207−214.
(21) Klauk, H.; Zschieschang, U.; Pflaum, J.; Halik, M. Ultralow-Power Organic Complementary Circuits. *Nature* **2007**, *445*, 745−748.
(22) Cattani-Scholz, A.; Pedone, D.; Blobner, F.; Abstreiter, G.; Schwartz, J.; Tornow, M.; Andruzzi, L. Pna-Peg Modified Silicon Platforms as Functional Bio-Interfaces for Applications in DNA Microarrays and Biosensors. *Biomacromolecules* **2009**, *10*, 489−496.
(23) Maxisch, M.; Thissen, P.; Giza, M.; Grundmeier, G. Interface Chemistry and Molecular Interactions of Phosphonic Acid Self-Assembled Monolayers on Oxyhydroxide-Covered Aluminum in Humid Environments. *Langmuir* **2011**, *27*, 6042−6048.
(24) Neves, B.; Salmon, M. E.; Russell, P. E.; Troughton, E. B. Spread Coating of Opa on Mica: From Multilayers to Self-Assembled Monolayers. *Langmuir* **2001**, *17*, 8193−8198.
(25) Metoki, N.; Liu, L.; Beilis, E.; Eliaz, N.; Mandler, D. Preparation and Characterization of Alkylphosphonic Acid Self-Assembled Monolayers on Titanium Alloy by Chemisorption and Electrochemical Deposition. *Langmuir* **2014**, *30*, 6791−6799.
(26) Wang, B.; Haick, H. Effect of Chain Length on the Sensing of Volatile Organic Compounds by Means of Silicon Nanowires. *ACS Appl. Mater. Interfaces* **2013**, *5*, 5748−5756.
(27) Knesting, K. M.; Ju, H.; Schlenker, C. W.; Giordano, A. J.; Garcia, A.; Smith, O. L.; Olson, D. C.; Marder, S. R.; Ginger, D. S. Ito Interface Modifiers Can Improve Voc in Polymer Solar Cells and Suppress Surface Recombination. *J. Phys. Chem. Lett.* **2013**, *4*, 4038−4044.
(28) Chockalingam, M.; Magenau, A.; Parker, S. G.; Parviz, M.; Vivekchand, S. R. C.; Gaus, K.; Gooding, J. J. Biointerfaces on Indium−Tin Oxide Prepared from Organophosphonic Acid Self-Assembled Monolayers. *Langmuir* **2014**, *30*, 8509−8515.
(29) Lange, I.; Reiter, S.; Pätzel, M.; Zykov, A.; Nefedov, A.; Hildebrandt, J.; Hecht, S.; Kowarik, S.; Wöll, C.; Heimel, G. Tuning the Work Function of Polar Zinc Oxide Surfaces Using Modified Phosphonic Acid Self-Assembled Monolayers. *Adv. Funct. Mater.* **2014**, *24*, 7014−7024.
(30) Timpel, M.; Nardi, M. V.; Krause, S.; Ligorio, G.; Christodoulou, C.; Pasquali, L.; Giglia, A.; Frisch, J.; Wegner, B.; Moras, P. Surface Modification of Zno (0001)− Zn with Phosphonate-Based Self-Assembled Monolayers: Binding Modes, Orientation and Work Function. *Chem. Mater.* **2014**, *26*, 5042−5050.
(31) Dubey, M.; Weidner, T.; Gamble, L. J.; Castner, D. G. Structure and Order of Phosphonic Acid-Based Self-Assembled Monolayers on Si (100). *Langmuir* **2010**, *26*, 14747−14754.
(32) Thissen, P.; Seitz, O.; Chabal, Y. J. Wet Chemical Surface Functionalization of Oxide-Free Silicon. *Prog. Surf. Sci.* **2012**, *87*, 272−290.
(33) Bashouti, M. Y.; Stelzner, T.; Christiansen, S.; Haick, H. Covalent Attachment of Alkyl Functionality to 50 Nm Silicon Nanowires through a Chlorination/Alkylation Process. *J. Phys. Chem. C* **2009**, *113*, 14823−14828.
(34) Puniredd, S. R.; Assad, O.; Haick, H. Highly Stable Organic Modification of Si(111) Surfaces: Towards Reacting Si with Further Functionalities While Preserving the Desirable Chemical Properties of Full Si−C Atop Site Terminations. *J. Am. Chem. Soc.* **2008**, *130*, 9184−9185.
(35) Puniredd, S. R.; Assad, O.; Haick, H. Highly Stable Organic Monolayers for Reacting Silicon with Further Functionalities: The Effect of the C−C Bond Nearest the Silicon Surface. *J. Am. Chem. Soc.* **2008**, *130*, 13727−13734.
(36) Levine, I.; Weber, S. M.; Feldman, Y.; Bendikov, T.; Cohen, H.; Cahen, D.; Vilan, A. Molecular Length, Monolayer Density, and Charge Transport: Lessons from Al−Alox/Alkyl−Phosphonate/Hg Junctions. *Langmuir* **2011**, *28*, 404−415.
(37) Bozzini, S.; Petrini, P.; Tanzi, M. C.; Zürcher, S.; Tosatti, S. Poly(Ethylene Glycol) and Hydroxy Functionalized Alkane Phosphate Mixed Self-Assembled Monolayers to Control Nonspecific Adsorption of Proteins on Titanium Oxide Surfaces. *Langmuir* **2009**, *26*, 6529−6534.
(38) Puniredd, S. R.; Srinivasan, M. P. Covalent Molecular Assembly in a Supercritical Medium: Formation of Nanoparticles Encapsulated in Immobilized Dendrimers. *Ind. Eng. Chem. Res.* **2007**, *46*, 464−471.
(39) Puniredd, S. R.; Srinivasan, M. P. Covalent Molecular Assembly of Oligoimide Ultrathin Films in Supercritical and Liquid Solvent Media. *Langmuir* **2005**, *21*, 7812−7822.
(40) Puniredd, S. R.; Srinivasan, M. P. Covalent Molecular Assembly of Multilayer Dendrimer Ultrathin Films in Supercritical Medium. *J. Colloid Interface Sci.* **2007**, *306*, 118−127.
(41) Puniredd, S. R.; Jayaraman, S.; Yeong, S. H.; Troadec, C.; Srinivasan, M. P. Stable Organic Monolayers on Oxide-Free Silicon/Germanium in a Supercritical Medium: A New Route to Molecular Electronics. *J. Phys. Chem. Lett.* **2013**, *4*, 1397−1403.
(42) Puniredd, S. R.; Zhang, F.; Srinivasan, M. P. Molecular Assembly of Materials with Covalent Bonding: Path to Robust Structures. *Mater. Sci. Eng., B* **2006**, *132*, 43−47.
(43) Zemanian, T. S.; Fryxell, G. E.; Liu, J.; Mattigod, S.; Franz, J. A.; Nie, Z. Deposition of Self-Assembled Monolayers in Mesoporous Silica from Supercritical Fluids. *Langmuir* **2001**, *17*, 8172−8177.
(44) Watkins, J. J.; McCarthy, T. J. Polymer/Metal Nanocomposite Synthesis in Supercritical Co2. *Chem. Mater.* **1995**, *7*, 1991−1994.
(45) Thissen, P.; Vega, A.; Peixoto, T.; Chabal, Y. J. Controlled, Low-Coverage Metal Oxide Activation of Silicon for Organic Functionalization: Unraveling the Phosphonate Bond. *Langmuir* **2012**, *28*, 17494−17505.
(46) Paska, Y.; Haick, H. Interactive Effect of Hysteresis and Surface Chemistry on Gated Silicon Nanowire Gas Sensors. *ACS Appl. Mater. Interfaces* **2012**, *4*, 2604−2617.
(47) McDermott, J. E.; McDowell, M.; Hill, I. G.; Hwang, J.; Kahn, A.; Bernasek, S. L.; Schwartz, J. Organophosphonate Self-Assembled Monolayers for Gate Dielectric Surface Modification of Pentacene-Based Organic Thin-Film Transistors: A Comparative Study. *J. Phys. Chem. A* **2007**, *111*, 12333−12338.
(48) Dubey, M.; Gouzman, I.; Bernasek, S. L.; Schwartz, J. Characterization of Self-Assembled Organic Films Using Differential Charging in X-Ray Photoelectron Spectroscopy. *Langmuir* **2006**, *22*, 4649−4653.
(49) Gouzman, I.; Dubey, M.; Carolus, M. D.; Schwartz, J.; Bernasek, S. L. Monolayer Vs. Multilayer Self-Assembled Alkylphosphonate Films: X-Ray Photoelectron Spectroscopy Studies. *Surf. Sci.* **2006**, *600*, 773−781.
(50) Nie, H.-Y.; McIntyre, N. S.; Lau, W. M.; Feng, J. M. Optical Properties of an Octadecylphosphonic Acid Self-Assembled Monolayer on a Silicon Wafer. *Thin Solid Films* **2008**, *517*, 814−818.
(51) Kanta, A.; Sedev, R.; Ralston, J. The Formation and Stability of Self-Assembled Monolayers of Octadecylphosphonic Acid on Titania. *Collod. Surf., A* **2006**, *291*, 51−58.
(52) Assad, O.; Leshansky, A. M.; Wang, B.; Stelzner, T.; Christiansen, S.; Haick, H. Spray-Coating Route for Highly Aligned and Large-Scale Arrays of Nanowires. *ACS Nano* **2012**, *6*, 4702−4712.
(53) Paska, Y.; Stelzner, T.; Assad, O.; Tisch, U.; Christiansen, S.; Haick, H. Molecular Gating of Silicon Nanowire Field-Effect Transistors with Nonpolar Analytes. *ACS Nano* **2011**, *6*, 335−345.

DOI: 10.1021/acsami.5b03597
ACS Appl. Mater. Interfaces 2015, 7, 14885−14895

(54) Wang, B.; Cancilla, J. C.; Torrecilla, J. S.; Haick, H. Artificial Sensing Intelligence with Silicon Nanowires for Ultraselective Detection in the Gas Phase. *Nano Lett.* **2014**, *14*, 933−938.
(55) Paska, Y.; Stelzner, T.; Christiansen, S.; Haick, H. Enhanced Sensing of Nonpolar Volatile Organic Compounds by Silicon Nanowire Field Effect Transistors. *ACS Nano* **2011**, *5*, 5620−5626.
(56) Du, J.; Liang, D.; Tang, H.; Gao, X. P. A. Inas Nanowire Transistors as Gas Sensor and the Response Mechanism. *Nano Lett.* **2009**, *9*, 4348−4351.
(57) Puniredd, S. R.; Srinivasan, M. P. Covalent Molecular Assembly in Supercritical Carbon Dioxide: A Comparative Study between Amine-and Anhydride-Derivatized Surfaces. *Langmuir* **2006**, *22*, 4092−4099.

DOI: 10.1021/acsami.5b03597
ACS Appl. Mater. Interfaces 2015, 7, 14885−14895